

Experimental Demonstration of Complex Image Theory for Vertical Magnetic Dipoles with Applications to Remote Sensing and Position Tracking

M. S. Trotter*

D. S. Ricketts[†]

J. D. Griffin*

Abstract — Position and orientation tracking in the magnetoquasistatic region of an electrically small transmitting loop antenna make use of complex image theory (CIT), which is an approximate algebraic model of the fields above a lossy dielectric, semi-infinite half-space. Experimental demonstrations of CIT from a transmitting loop that approximates a horizontal magnetic dipole (HMD) have been reported previously. This work reports the first experimental demonstration of CIT from a vertical magnetic dipole (VMD) in remote sensing and position-tracking applications.

1 INTRODUCTION

Low frequency position tracking and remote sensing require the accurate measurement and modeling of magnetoquasistatic fields. In such applications, an interface between air and a lossy dielectric, such as the earth’s surface, are often encountered, which complicates the analytical calculation of the fields. While closed-form analytical solutions and Finite Element Modeling (FEM) solvers can both produce accurate calculations of fields, they are typically computationally intensive and are not suitable for many tracking and sensing applications where limited computational infrastructure exists or analysis must be done in a very short time. Two examples of these are the tracking of an American football during a game [1] and remote sensing by vehicles for landing [2].

In this work, we report the first experimental demonstration of complex image theory to easily and accurately model the fields generated by a vertical magnetic dipole in remote sensing and position tracking applications. We also show that any measured range estimation is due to the discrepancy between complex image theory (CIT) and the exact integral solution for the fields. Section 2 provides background on CIT, which is an algebraic model for the fields from magnetic dipole source above a semi-infinite conducting half-space. Sec-

tion 3 describes the experimental setup for measuring the fields from a vertical magnetic dipole (VMD). Lastly, Section 4 gives a comparison of theoretical models and an investigation of the accuracy of range estimation using CIT.

2 BACKGROUND

The complex image theory (CIT) model, derived by Wait [3] and Weaver [4], is an algebraic approximation to the exact Sommerfeld solution [5] for the magnetoquasistatic fields emitted by a magnetic dipole above a lossy half space. Fig. 1a shows the geometry for the situation where the transmitter is in air above loamy soil commonly found in fertile lands of the USA. The rules for reflection of a magnetic dipole above a reflective ground plane are given as well [6]. CIT combines the flux density from the magnetic dipole source at height h above the earth with the flux density from the magnetic dipole image at the complex-valued depth $h + \delta(1 - j)$ into earth, where δ is the skin depth $\delta = \sqrt{2/\omega\mu\sigma}$. The flux density from complex image theory is

$$\vec{B}_{\text{CIT}}(x, y, z) = \vec{B}(\vec{R}_0, \vec{m}_s) + \vec{B}(\vec{R}_2, \vec{m}_{\text{im}}), \quad (1)$$

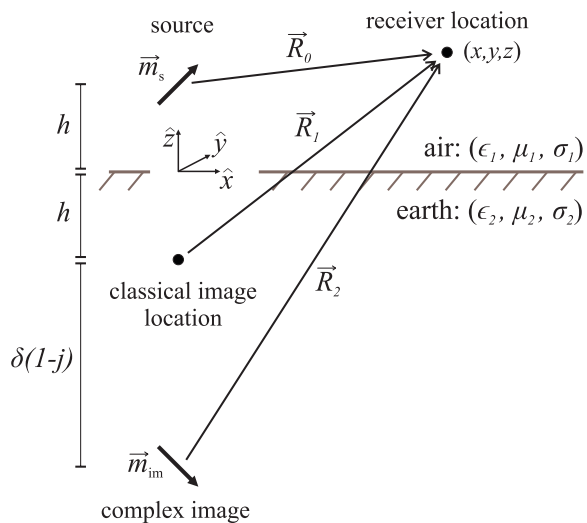
where the equation for the flux density \vec{B} from a time-harmonic magnetic dipole source is [7]

$$\begin{aligned} \vec{B}(\vec{R}_0, \vec{m}_s) = & \\ & \frac{-k^3\mu_0}{4\pi} \left\{ \left[\frac{1}{(kR_0)^3} + \frac{j}{(kR_0)^2} \right] (1 - 3\hat{R}_0\hat{R}_0 \cdot) \vec{m}_s \right. \\ & \left. + \left(\frac{1}{kR_0} \right) \hat{R}_0 \times (\hat{R}_0 \times \vec{m}_s) \right\} e^{-jkR_0}. \end{aligned} \quad (2)$$

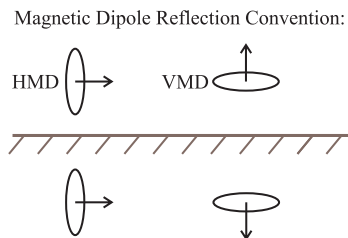
Here, \vec{R}_0 is the distance vector from the magnetic dipole source to the observation point (x, y, z) . The magnetic dipole moment of the source is \vec{m}_s and of the image is \vec{m}_{im} . CIT differs from classical image theory in the location of the image; for classical image theory, the image depth is h below the surface of the earth instead of $h + \delta(1 - j)$ for CIT. This fact modifies the magnitude of the distance between the receiver and the image and introduces

*Disney Research, Pittsburgh, Pennsylvania, USA, e-mail: mtrotter@disneyresearch.com, joshdgriffin@disneyresearch.com

[†]NC State, Raleigh, North Carolina, USA, e-mail: david.ricketts@ncsu.edu



(a)



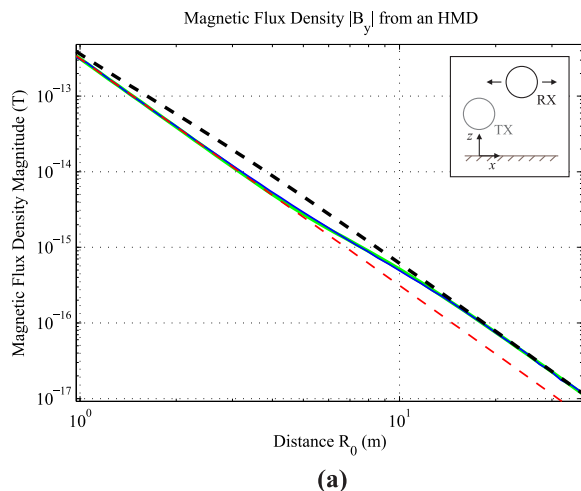
(b)

Figure 1: (a) Geometry for a transmitting loop of current above a semi-infinite earth. (b) Convention for image orientations of magnetic dipole sources.

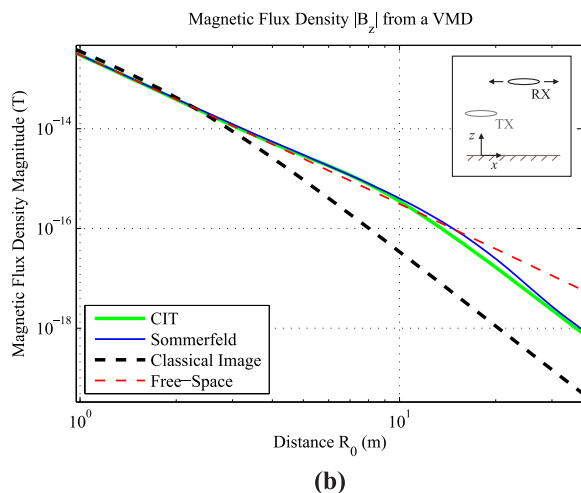
a phase shift; CIT uses R_2 as the image distance to the receiver, and classical image theory uses R_1 as the image distance.

The VMD transmitter measured in this paper behaves differently from the HMD source studied previously [1]. As shown in Fig. 1b, the image from an HMD is not inverted and therefore provides constructive interference to the fields of the HMD transmitter. The z -component of the image from a VMD is inverted, however, which produces fields that destructively interfere with the fields of the VMD transmitter. The effects of the image inversion can be seen in Fig. 2, where the flux density decays much faster ($1/R_0^5$) for the VMD than for the HMD orientation ($1/R_0^3$). Furthermore, the classical image theory serves as an asymptotic limit for CIT at long ranges for the HMD. The VMD case shows that, while both decay at the same rate, CIT does not asymptotically approach classical image theory.

Agreement between models changes at close and middle ranges as well. At close ranges (i.e. $R_0 \ll$



(a)



(b)

Figure 2: Theory comparison for the (a) HMD transmitter orientation and (b) VMD transmitter orientation.

R_2), all models converge to match the free-space model, which is expected since image contributions are negligible at close range. In middle ranges (i.e. $R_0 \sim R_2$), CIT and the exact Sommerfeld models match closely but differ from classical image theory and free-space theory.

3 EXPERIMENTAL SETUP

A visual diagram of the placement and orientations of the transmitter and receiver as well as corresponding circuit diagrams are shown in Fig. 3a. A transmitting loop antenna was placed 87.5 cm above a flat, grassy field such that its surface normal pointed perpendicular to the earth and thus approximated a VMD. The circuit diagrams of the transmitter and receiver are shown in Fig. 3b. The loop consisted of 45 turns of 35 AWG copper wire around a nonmagnetic core with a diameter of

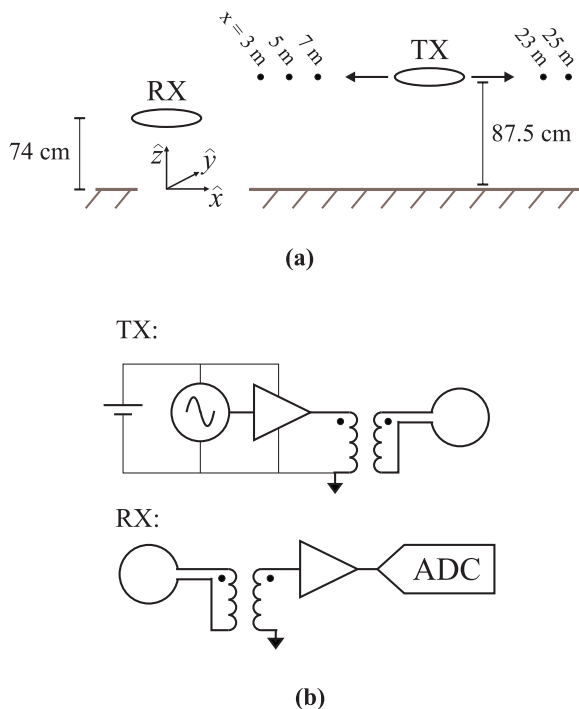


Figure 3: (a) The transmitter was measured along a trajectory parallel to the x -axis in 2-m increments. (b) Block diagram of transmitting and receiving hardware. MATLAB was used as the post-processing software.

16.5 cm and driven by a 0.5 W class E oscillator at a frequency of 348 kHz. A 3.7 V Lithium Polymer battery provided DC power to the transmitter and amplifier. The z -component of the magnetic field was measured with a Wellbrook LFL-1010 active receiving loop with a diameter of 1 m. An Adlink PXI-9816 analog-to-digital converter (ADC) was used to digitize the received waveform at a sampling rate of 5 MHz. MATLAB was used to process all received data and provide range estimations.

Fig. 4 shows the outdoor measurement setup. The vertically oriented transmitter was moved along the x -axis from $x = 3$ to 25 m in 2 m increments. The z -component of the flux density was measured with the vertically oriented receiver fixed over the origin at a height of 74 cm.

4 RESULTS AND DISCUSSION

Fig. 5a shows the measured flux density at each location and also shown are the fields calculated from the free-space model, classical image theory, CIT, and the exact solution (numerically solved using the Sommerfeld integral equation at each point). The conductivity of the earth was determined by a best fit of the exact solution to the measured data as $\sigma = 0.05$ S/m, which is within the expected range for the loamy soil at the test site [8]. This value of conductivity was used for the CIT model as well;

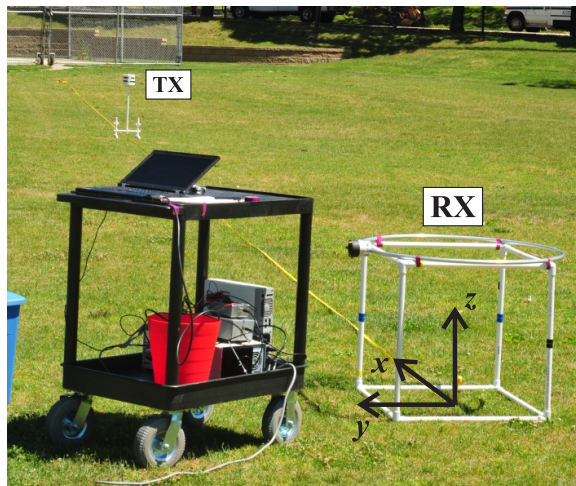


Figure 4: The TX was moved along the x -axis in over the grassy field from $x = 3$ to 25 m while the RX stayed in a fixed location above the origin at a height of 74 cm.

the free-space and classical image theory models do not make use of the earth conductivity. The measurements follow the free-space model out to a distance of approximately 15 m, where the complex image becomes significant. Here, the field falls with a similar trend to classical image theory but at a significant offset. The experimental measurements show that, while the Sommerfeld solution is the best fit, CIT provides an accurate model of the fields above the earth with the advantage of less computational expense than the Sommerfeld solution.

Fig. 5b shows the distance estimation error calculated by inverting the field equations [1]. The series labeled “Meas. Error from Sommerfeld Model” shows the distance estimation error using the Sommerfeld exact integral as a model for the measured fields. Specifically,

$$x' = \left\{ \chi : \vec{B}_{\text{ex}}(\chi, y, z) = \vec{B}_{\text{meas}}(x, y, z) \right\}, \quad (3)$$

where (x, y, z) is the true location of the transmitter during measurement, and χ is the tested x -value of range in the exact Sommerfeld model \vec{B}_{ex} . The resulting estimation error is the difference $x' - x$. Since the Sommerfeld model represents the exact solution for the magnetic flux density above a conducting half-space (i.e., earth), we attribute the errors to experimental inaccuracies such as variations in the orientation of the TX and RX loops, inhomogeneous earth conductivity, buried objects, noise, and a non-flat earth (Fig. 4).

The series labeled “Meas. Error from CIT Model” shows the distance estimation error using the CIT model. The error is larger than with the Sommerfeld model as might be expected since CIT

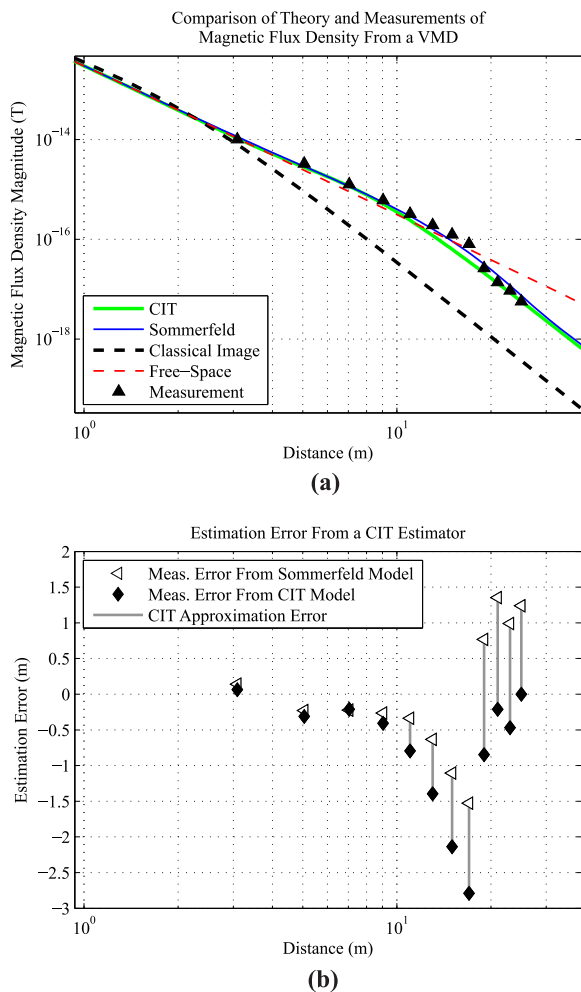


Figure 5: (a) Measured values of flux density $|B_z|$ compared with theory. (b) Measured estimation error of the x value of the transmitter. The portion of estimation error due to the CIT approximation is also plotted.

is an approximation to the Sommerfeld model. To show that the error is due to the difference between CIT and Sommerfeld, we calculated the theoretical estimation error that arises due to the CIT approximation of the Sommerfeld model. We represent these calculated errors by the grey vertical bars in Fig. 5b. We placed the starting point of each bar on the “Meas. Error from Sommerfeld Model” to see if the measurement error and CIT approximation error would equal the estimation error shown by the series “Meas. Error from CIT”. From Fig. 5b, we can see that it does indeed, and thus the estimation error for the CIT model is the sum of the experimental and CIT approximation error.

The estimation error using the CIT model is significantly higher than reported in [1], where the peak-to-peak error for the HMD was 0.4 m. In contrast, this current work shows a peak-to-peak error of 2.85 m. We attribute the increased error

for the VMD case to the combination of increased experimental error over [1] and an increased error in the CIT approximation of Sommerfeld for the VMD. The error due to the CIT approximation depends on the conductivity and operating frequency and, thus, is not uniform for all possible cases; in some instances the error could be smaller or larger depending on the frequency and conductivity.

5 CONCLUSIONS

This work presented the first experimental measurements of range estimation error arising from a vertical magnetic dipole transmitter. The estimation error (2.85 m) was found to be larger than a previous measurement of the estimation error (0.4 m) from a horizontal magnetic dipole transmitter. The larger error arises due to the large disparity between CIT and the exact Sommerfeld integral theory.

References

- [1] D. D. Arumugam, J. D. Griffin, and D. D. Stancil, “Experimental demonstration of complex image theory and application to position measurement,” *IEEE Antennas and Wireless Propagation Letters*, vol. 10, pp. 282–285, 2011.
- [2] D. Arumugam, D. Stancil, and D. Ricketts, “Proximity and orientation sensing using magnetoquasistatic fields and complex image theory,” in *Vehicle Technology Conference (VTC Fall), 2011 IEEE*, 2011, pp. 1–5.
- [3] J. R. Wait and K. P. Spies, “On the image representation of the quasi-static fields of a line current source above the ground,” *Canadian Journal of Physics*, vol. 47, pp. 2731–2733, 1969.
- [4] J. T. Weaver, “Image theory for an arbitrary quasi-static field in the presence of a conducting half space,” *Radio Science*, vol. 6, pp. 647–653, 1971.
- [5] A. Sommerfeld, “Über die ausbreitung der wellen in der drahtlosen telegraphie,” *Annalen der Physik*, pp. 665–736, 1909.
- [6] C. Balanis, *Antenna Theory, Analysis and Design*. John Wiley and Sons, 2005.
- [7] G. S. Smith, *An Introduction to Classical Electromagnetic Radiation*. Cambridge University Press, 1997.
- [8] A. R. von Hippel, *Dielectric Materials and Applications*. M.I.T. Press, 1954.